blood®
Regular Article

IMMUNOBIOLOGY AND IMMUNOTHERAPY

Immunoglobulin light-chain toxicity in a mouse model of monoclonal immunoglobulin light-chain deposition disease

Sébastien Bender,[1,2] Maria Victoria Ayala,[1,*] Amélie Bonaud,[3,*] Vincent Javaugue,[1,2,4] Claire Carrion,[1] Christelle Oblet,[1] Alexia Rinsant,[2] Sihem Kaaki,[2,5] Zeliha Oruc,[1] François Boyer,[1] Agnès Paquet,[6] Nicolas Pons,[6] Bastien Hervé,[7] Mohamad Omar Ashi,[1] Arnaud Jaccard,[1,2,8] Laurent Delpy,[1] Guy Touchard,[4] Michel Cogné,[1,9] Frank Bridoux,[1,2,4] and Christophe Sirac[1,2]

[1]Unité Mixte de Recherche (UMR) 7276/INSERM U1262, Centre National de la Recherche Scientifique (CNRS), Université de Limoges, Limoges, France; [2]Centre National de l'Amylose AL et Autres Maladies par Dépôt d'Immunoglobulines Monoclonales, Centre Hospitalier Universitaire de Limoges, Limoges, France; [3]INSERM U1160, Institut de Recherche Saint-Louis, Saint Louis Hospital, Paris, France; [4]Service de Néphrologie et Transplantation, Centre Hospitalier Universitaire de Poitiers, Poitiers, France; [5]Service de Pathologie et de Pathologie Ultrastructurale, Centre Hospitalier Universitaire de Poitiers, Poitiers, France; [6]Institut de Pharmacologie Moléculaire et Cellulaire, CNRS, Université Côte d'Azur, Sophia-Antipolis, France; [7]Plateform Biologie Intégrative Santé Chimie Environnement, Université de Limoges, Limoges, France; [8]Service d'Hématologie Clinique, Centre Hospitalier Universitaire de Limoges, Limoges, France; and [9]Institut Universitaire de France, Paris, France

KEY POINTS

- **Human pathogenic immunoglobulin LC fully reproduces LCDD in a transgenic mouse, including glomerulosclerosis and end-stage renal failure.**
- **In addition to its kidney toxicity, LCDD LC induces endoplasmic reticulum stress and sensitizes PCs to proteasome inhibitors.**

Light chain (LC) deposition disease (LCDD) is a rare disorder characterized by glomerular and peritubular amorphous deposits of a monoclonal immunoglobulin LC, leading to nodular glomerulosclerosis and nephrotic syndrome. We developed a transgenic model using site-directed insertion of the variable domain of a pathogenic human LC gene into the mouse immunoglobulin κ locus, ensuring its production by all plasma cells (PCs). High free LC levels were achieved after backcrossing with mice presenting increased PC differentiation and no immunoglobulin heavy chain production. Our mouse model recapitulates the characteristic features of LCDD, including progressive glomerulosclerosis, nephrotic-range proteinuria, and finally kidney failure. The variable domain of the LC bears alone the structural properties involved in its pathogenicity. RNA sequencing conducted on PCs demonstrated that LCDD LC induces endoplasmic reticulum stress, likely accounting for the high efficiency of proteasome inhibitor–based therapy. Accordingly, reduction of circulating pathogenic LC was efficiently achieved and not only preserved renal function but also partially reversed kidney lesions. Finally, transcriptome analysis of presclerotic glomeruli revealed that proliferation and extracellular matrix remodeling represented the first steps of glomerulosclerosis, paving the way for future therapeutic strategies in LCDD and other kidney diseases featuring diffuse glomerulosclerosis, particularly diabetic nephropathy. (*Blood*. 2020;136(14):1645-1656)

Introduction

Monoclonal gammopathies of renal significance (MGRSs) are characterized by renal lesions resulting from monoclonal immunoglobulins produced by a nonmalignant B- or plasma-cell (PC) clone.[1] They comprise tubulopathies caused by light chain (LC) accumulating in the proximal or distal tubules, or glomerulopathies, most frequently amyloid LC (AL) amyloidosis and Randall-type monoclonal immunoglobulin deposition disease (MIDD).[2] MIDDs are characterized by linear amorphous deposits of a monoclonal LC (LC deposition disease [LCDD]) or a truncated heavy chain (HC; HC deposition disease [HCDD]) along the tubular and glomerular basement membranes (BMs), around arteriolar myocytes, and in the mesangium, eventually leading to diabetic-like nodular glomerulosclerosis. Clinical manifestations include glomerular proteinuria with progressive kidney failure.[3-5]

In LCDD, the most frequent form of MIDD, involved LCs are mostly of the κ isotype, with a striking overrepresentation of the Vκ4 variable (V) domain. Cationic V domains and/or complementarity-determining regions could account for their propensity to deposit along negatively charged BMs.[5-7] However, little is known about the pathogenic mechanisms involved in glomerular damage leading to proteinuria and glomerulosclerosis. Russell et al,[8] Keeling et al,[9,10] and Herrera et al[11] showed the acquisition of a myofibroblast phenotype by mesangial cells exposed to purified LCDD LC. As in diabetic nephropathy (DN),[12] these changes occurred along with the increased production of platelet-derived growth factor β (PDGFβ) and transforing growth factor β (TGFβ), resulting in excessive generation of extracellular matrix (ECM) proteins. However, because most of these experiments relied on acute

exposure to pathogenic LC, they should be confirmed in a model reproducing the progressive development of glomerular lesions observed in MIDD. We recently developed a transgenic mouse model of MIDD in which the continuous production of a truncated HC from an HCDD patient by PCs led the main pathologic features of HCDD, but neither glomerulosclerosis nor kidney dysfunction was observed.[13] In the present study, we developed a transgenic mouse model of LCDD (double homozygous DH-LMP2A [DH] and κF strain [κF-DH]) using targeted insertion of a human LC gene into the mouse κ locus, coupled with a deletion of the HC genes, to obtain high levels of circulating pathogenic free LC (FLC).[14] This strategy proved efficient, with the induction of full-blown LCDD, and provided new insights into the pathophysiology of the disease and into the toxicity of monoclonal LC for PCs.

Methods

Mice

Gene targeting into the murine immunoglobulin κ locus was performed as previously described.[15] The procedure is detailed in the supplemental Methods (available on the *Blood* Web site) and Figure 1A. As described elsewhere[14] and in the supplemental Methods, LC transgenic mice (κF) were backcrossed with the DH strain to produce only free LC (Figure 1A). LCDD mice, corresponding to κF-DH were analyzed throughout this study. Primers used are listed in supplemental Table 1. DH mice[16] were kindly provided by S. Casola (Istituto FIRC di Oncologia Molecolare, Milan, Italy). All animals had a mixed genetic background (BALB/C × 129SV × C57/BL6) and were maintained in pathogen-free conditions and analyzed at 2, 6, and 8 months except when otherwise stated. All experimental procedures were approved by our Institutional Review Board for Animal Experimentation, and by the French Ministry of Research (#7655-2016112211028184).

In vivo treatment, surgery, and biochemical parameters

For long-term treatment, mice were treated with 0.75mg/kg of bortezomib[13,17] (Velcade; Janssen Cilag) and 2 mg/kg of cyclophosphamide (Endoxan; Baxter) once per week over 2 months. Bortezomib was injected subcutaneously, and cyclophosphamide was injected intraperitoneally. To test the sensitivity of PCs to proteasome inhibitor (PI), we injected for 2 consecutive days a suboptimal dose of bortezomib as previously described.[13] Biochemical parameters were measured on a Konelab 30 analyzer with a creatinine enzymatic test (Thermo Fisher Scientific). Urine albumin concentrations were measured using a mouse albumin enzyme linked immunosorbent assay (ELISA) kit (Abcam).

Pathologic studies, ELISA, and western blot analysis

Kidney samples were processed for light microscopic examination, immunofluorescence, and electron microscopic studies as previously described.[13] Some specific techniques and the lesion score protocol are described in the supplemental Methods. Serum was analyzed for the presence of κLC by ELISA and western blots as previously described.[13,15] Antibodies are listed in supplemental Table 2.

Glomeruli extraction

Isolation of kidney glomeruli from mice was derived from Takemoto et al.[18] Briefly, mice were perfused in the heart with magnetic Dynabeads 4.5 μm in diameter. Kidneys were minced, digested by Dnase I (Roche) and collagenase IV (Sigma-Aldrich), and filtered, and glomeruli were isolated using a magnetic rack. We could not apply this technique to kidneys with advanced sclerosis, because of the lack of access of the beads to the glomerular capillaries.

Flow cytometry and PC enrichment

Intracellular staining was performed using the Intraprep Kit (Beckman Coulter). Flow cytometric analysis was performed on a BD Pharmingen LSRFortessa cytometer. Data were analyzed with BD FACSDiva software (BD Biosciences). PC enrichment was performed using a mouse CD138$^+$ PC Isolation Kit (Miltenyi Biotec).

Transcriptional analysis

Total RNA from purified glomeruli or PCs was obtained using the miRNeasy Mini Kit (Qiagen), and purity (RNA integrity number >7) was assayed with the Bioanalyzer RNA 6000 Nano (Agilent). RNA sequencing (RNA-seq) libraries were generated with 500 ng of RNA. Alternatively, reverse transcription was performed using a high-capacity complementary DNA (cDNA) Reverse Transcription Kit (Applied Biosystems), with random hexamers. Relative quantification was performed with Premix Ex Taq or SYBR Premix Ex Taq (Takara) on cDNA samples (10 ng per reaction). Quantification of the gene of interest was analyzed by the ΔCt method, with immunoglobulin J used as the housekeeper gene. Probes are listed in supplemental Table 1.

RNA-seq

Libraries were generated from 500 ng of total RNA using the Truseq Stranded mRNA Kit (Illumina), quantified with the Qubit dsDNAHS Assay Kit (Invitrogen), and pooled; 4 nM of this pool were loaded on a Nextseq 500 high-output flow cell and sequenced on a NextSeq 500 platform (Illumina) with 2 × 75–bp paired-end chemistry. Bioinformatic pipelines for mapping and filtering and tools for pathways analysis are described in the supplemental Methods. Gene Expression Omnibus accession numbers for the RNA-seq data sets reported in this paper are as follows: GSE119049 for glomeruli and GSE119048 for PCs (Gene Expression Omnibus superseries GSE119050).

Statistical analysis

The statistical tests used to evaluate differences between variables were carried out using Prism software (GraphPad Software). Statistical significance was determined using the nonparametric Mann-Whitney test to assess 2 independent groups and the log-rank (Mantel-Cox) test for survival analyses. Values of $P < .05$ were considered significant.

Results

Efficient transgenic strategy to produce high amounts of human pathogenic LC in mice

LCDD mice, as described in "Methods" (Figure 1A-B), closely recapitulate the features of monoclonal gammopathy, with an elevated number of PCs producing the human/mouse chimeric monoclonal FLC. Indeed, LCDD mice presented with ~10% of

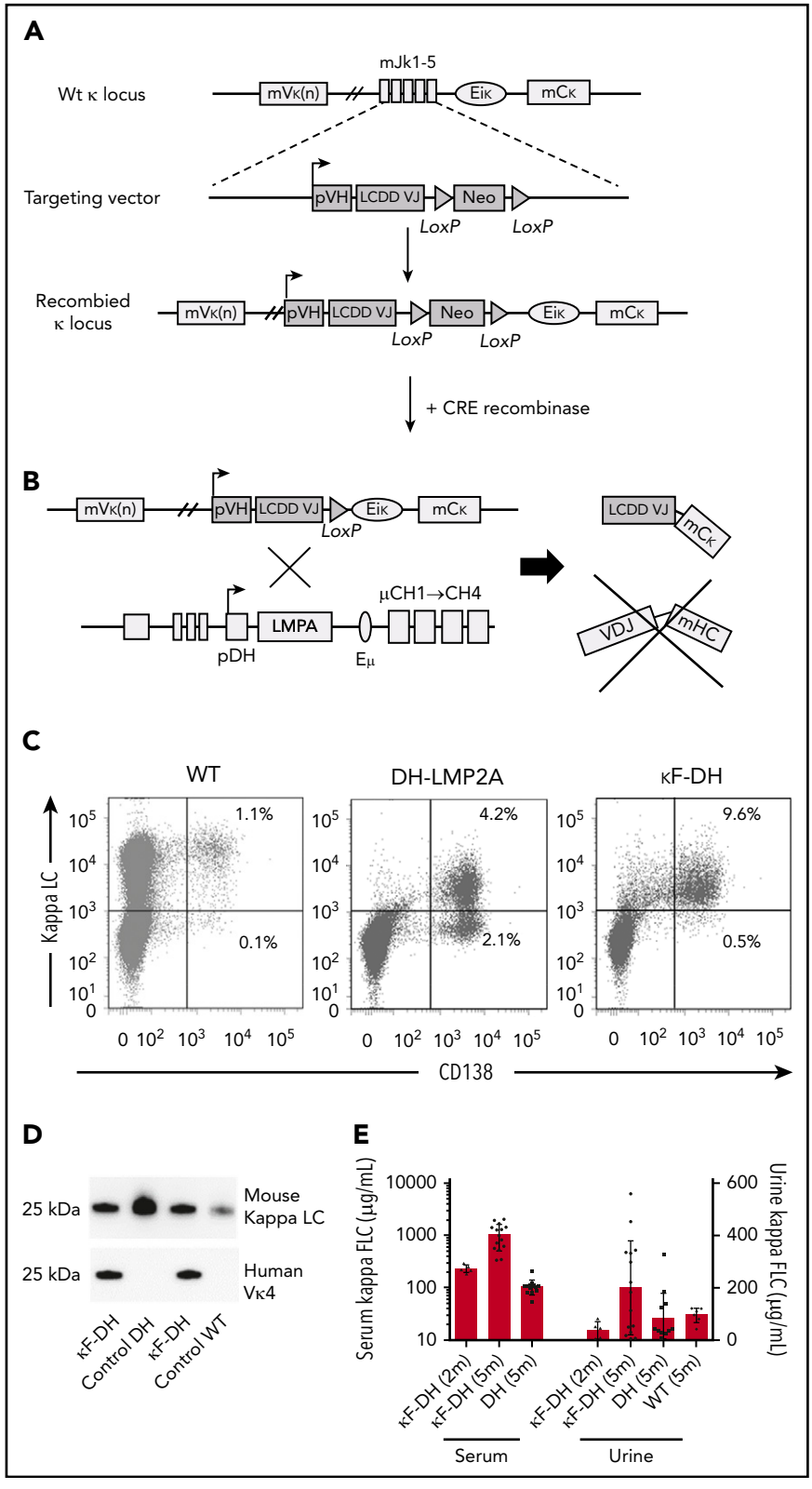

Figure 1. Strategy to produce high amounts of a human κLC in mice. (A) The strategy consists of replacing the Jκ segments in a wild-type (WT) unrearranged mouse κ locus by a human VJ exon/neomycin cassette. The absence of the Jκ segments in the newly recombined κ locus blocks all possibilities of endogenous rearrangements. A Cre-mediated deletion of the neomycin resistance gene leads to the production of a chimeric human VJ/mouse κ constant LC. (B) Breeding with DH mice enables the production of only FLC by B cells and PCs. (C) Flow cytometric analysis of PCs isolated from spleen and stained with anti-mouse CD138 and anti-mouse κ antibodies. Note the increase of PCs in DH models compared with WT and that nearly all PCs are κ^+/$CD138^+$ in κF-DH mice. (D) Western blot analysis of the produced κLC in sera of κF-DH, DH, and WT mice with anti-mouse κ antibody (top) and anti-human Vκ4 V domain (bottom). The bands appear at the expected size of 25 kDa, and anti-human Vκ4 antibody reveals only the chimeric κLC of the κF-DH mice. (E) Serum and urine levels (in μg/mL) of κFLC in 2- and 5-month-old κF-DH mice compared with 5-month-old DH and WT mice. The κFLC levels increase in κF-DH mice with age. Serum results are expressed in log scale; means ± standard error of the mean.

PCs in spleen (as compared with ~1% in WT mice), of which 95% produced the transgenic LC (Figure 1C-D). Serum FLC levels were similar to those observed in patients with LCDD,[19] progressively increased with age, and lasted the lifespan of the animals. Bence-Jones proteinuria was readily detectable in 5-month-old mice (Figure 1E).

Severe kidney failure induces premature death of LCDD mice

κF-DH mice (n = 12 in 2 independent cohorts) were monitored daily from month 5 for external signs of morbidity (see "Methods"). Median survival was 8.5 months, with the first mouse euthanized at

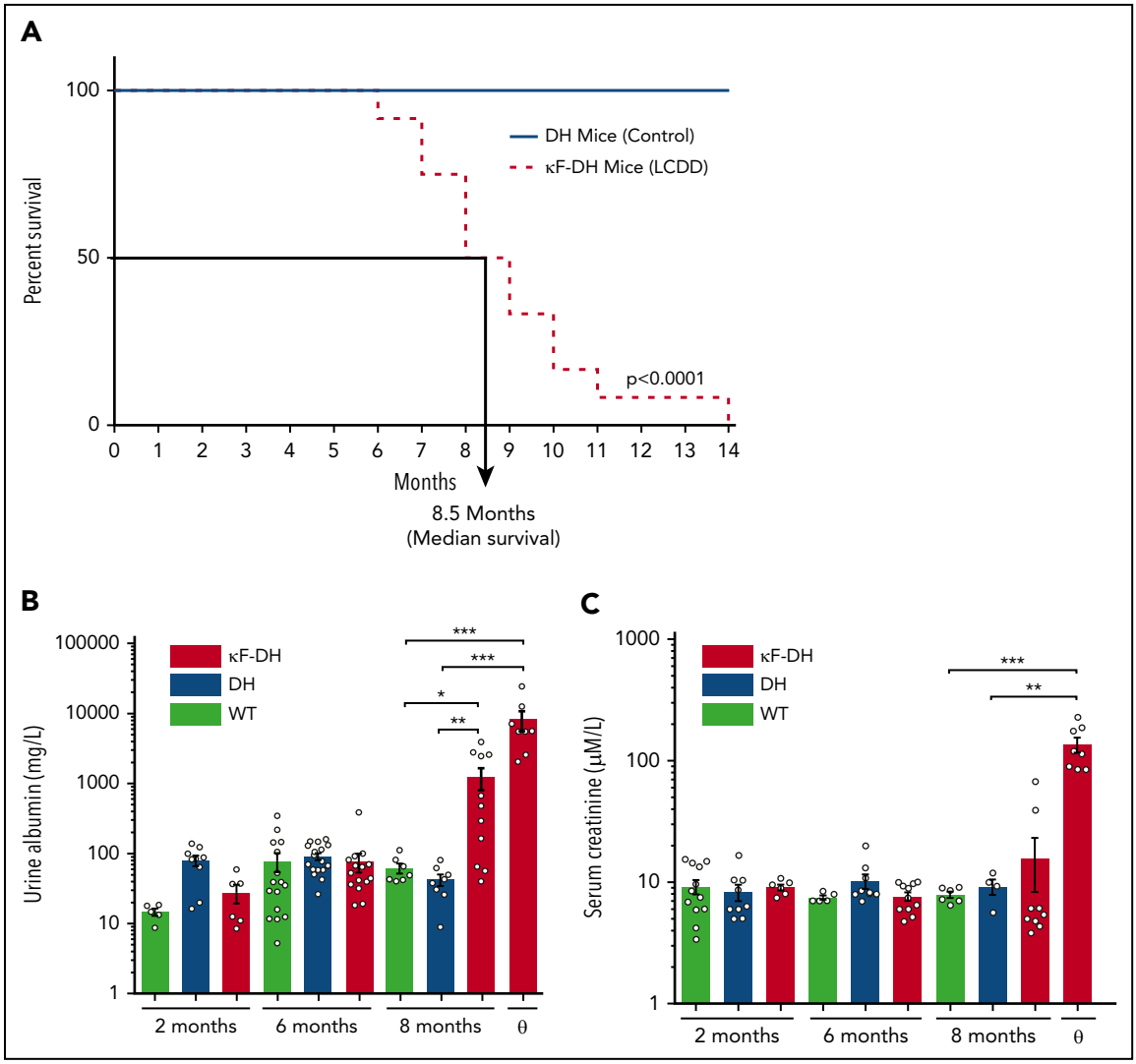

Figure 2. Survival analysis and kidney function in κF-DH mice. (A) Kaplan-Meier overall survival analysis of κF-DH mice (n = 12) compared with DH mice (n = 10). Note the short 8.5-month median survival for κF-DH mice compared with DH mice (all alive at 14 months). Urine albumin (B) and serum creatinine levels (C) in 2- to 8-month-old κF-DH, DH, and WT mice and in κF-DH mice at humane end point (θ). Urine albumin in κF-DH mice started to increase at 8 months, whereas a strong increase of serum creatinine appeared only in unhealthy mice. Survival data were analyzed using log-rank (Mantel-Cox) test, and comparisons between 2 groups were calculated using the nonparametric Mann-Whitney test. Means ± standard error of the mean, and only significant *P* values are indicated. $*P < .05$, $**P < .01$, $***P < .001$.

6 months and the last at 14 months (Figure 2A). DH mice (n = 10 in 2 independent cohorts) were used as control (similarly to κF-DH mice, they do not produce complete antibodies). At 14 months, all control mice were healthy (Figure 2A). Increased albuminuria was observed in 8-month-old κF-DH mice (Figure 2B). Mice euthanized at humane end points showed heavy albuminuria, reaching up to 24.80 g/L (mean, 8.30 ± 2.63 g/L; Figure 2B), together with high serum creatinine (135.58 ± 19.23 vs 7.89 ± 0.47 and 9.20 ± 1.33 μM/L in 8-month-old WT and DH control mice, respectively), confirming severe kidney failure in these mice (Figure 2C). Macroscopic observations revealed pale and atrophic kidneys (supplemental Figure 1). Altogether, these results confirm that the short lifespan of κF-DH mice is due to end-stage renal failure.

Pathogenic human LC recapitulates renal lesions of LCDD

Pathologic studies were carried out in 2- and 6-month-old κF-DH mice and in mice euthanized at humane end points. As early as 2 months, immunofluorescence analysis revealed linear LC deposits along glomerular (Figure 3A) and medullary tubule BMs (supplemental Figure 2). At 6 months of age, intense LC staining was observed along all BMs in the renal medulla and cortex and into the mesangial space of glomeruli (Figure 3A; supplemental Figure 2), but kidneys showed normal tubular and glomerular structures (Figure 3A; supplemental Figure 2). In contrast, mice euthanized at humane end points displayed an absence of detectable LC reabsorption in proximal tubules, with massive staining of tubular BMs, mesangium, and Bowman's capsule and diffuse nodular appearance of glomerular deposits (Figure 3A; supplemental Figure 2). Corticomedullary dedifferentiation suggestive of severe renal failure was observed (supplemental Figure 2). Periodic acid Schiff staining confirmed thickening of tubular BMs, mesangial extracellular matrix expansion with mesangial cell proliferation and mesangiolysis, and nodular glomerulosclerosis with glomeruli enlargement (Figure 3B). Focal areas of interstitial fibrosis with inflammatory infiltrates

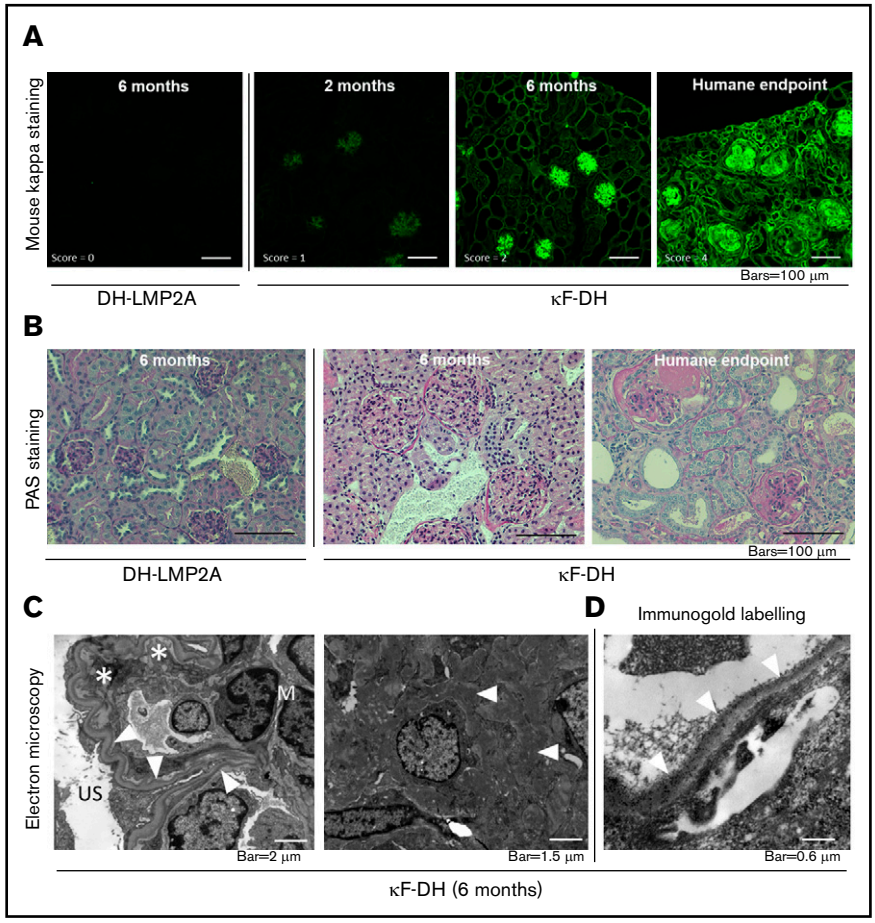

Figure 3. Kidney section analysis of κF-DH mice. (A) Immunofluorescence microscopy on frozen kidney sections of κF-DH mice using anti-mouse κ antibody at 2 and 6 months and humane end point, compared with DH control mice. κLC deposits in κF-DH mice are detectable as soon as age 2 months and become intense with age along tubular and glomerular BMs and in the mesangium. Lesion scores are indicated (see "Methods"). Original magnification ×200. (B) Periodic acid Schiff (PAS) staining performed on paraffin-embedded kidney sections showing tubular BMs thickening and nodular glomerulosclerosis with mesangial expansion of the ECM and mesangial cell proliferation. Note the massive enlargement of glomeruli in κF-DH mice. Original magnification ×200. (C) Electron microscopic analysis showing in left panel linear electron-dense deposits in the inner aspect of the glomerular BM (arrowhead). Subendothelial space is extremely widened, consistent with thrombotic microangiopathy–like lesions (asterisk). Original magnification ×8000. Right panel shows granular electron-dense deposits in the mesangium (arrowhead). Original magnification ×10 000. (D) Immunoelectron microscopy (original magnification ×40 000). Presence of anti-κ gold-conjugated particles along the inner aspect of glomerular BM (arrowhead). All data are representative of at least 3 kidneys in each group.

mainly composed of granulocytes/macrophages (CD11b$^+$) and T cells (CD3$^+$; supplemental Figure 3) were observed around sclerotic glomeruli and dilated tubules (Figure 3B). Electron microscopy revealed characteristic linear powdery punctuate deposits on the inner aspect of glomerular BMs and the outer aspect of tubular BMs, diffuse thickening of tubular and glomerular BMs, and expanded mesangial areas with massive accumulation of electron-dense material (Figure 3C). Finally, immunoelectron microscopy using gold-labeled anti-mouse κLC confirmed the κ composition of the deposits (Figure 3D). Lesions of thrombotic microangiopathy with widening of the subendothelial zone by electron lucent material were seen in some glomeruli from 6-month-old mice and in most glomeruli from mice euthanized at humane end points (Figure 3C-D). Similarly to the patient from whom the LC gene was extracted,[20] κF-DH mice also yielded LC deposits in other organs, including lung, liver, and heart (supplemental Figure 4). Collectively, kidney lesions observed in κF-DH mice fully recapitulate the human pathologic features of MIDD and are consistent with premature death resulting from end-stage kidney failure.

Early induction of cell-cycle and ECM remodeling is involved in LC-induced glomerulosclerosis

Having demonstrated that most 6-month-old κF-DH mice presented with early renal lesions of LCDD (Figure 3), we sought to compare their glomeruli transcriptome with that of control mice. RNA-seq performed on purified glomeruli revealed a total of 360 and 475 genes expressed differentially in κF-DH mice compared with WT and DH controls, respectively (abs[$\log_2$FC] ≥0.7, false discovery rate (FDR) ≤0.05; Figure 4A; supplemental Figure 5A). Among these genes, 192 were deregulated compared with both controls, with 155 upregulated and 37 downregulated genes (supplemental Figure 5A-B). We performed a C2 canonical pathway analysis from the Molecular Signatures Database (MSignDB v.6.2),[21,22] which revealed that the cell cycle (mitotic) was the main modified pathway (Figure 4B; supplemental Table 3). All deregulated genes involved in the cell cycle were upregulated (Figure 4A; supplemental Figure 5A-B; supplemental Table 3). In addition to the cell cycle, we found 24 deregulated genes involved in the matrisome pathway (upregulated, n = 18; downregulated, n = 6), including the previously described upregulation of tenascin C (Tnc) and CTGF, known to be involved in glomerulosclerosis and interstitial fibrosis (Figure 4A-B; supplemental Figure 5B; supplemental Table 3).[10,12,23] However, we did not find any activation of pathways related to TGFβ, despite its established role in glomerulosclerosis. Immunostaining for Ki67 (Figure 4C-D) and Tnc (supplemental Figure 6) in 6-month-old mice confirmed extensive cell-cycle and ECM remodeling, respectively, in the glomeruli of κF-DH mice.

LCDD LC induces ER stress and sensitizes PCs to PIs

Several studies have demonstrated that the production of a pathogenic monoclonal immunoglobulin or immunoglobulin fragment could influence PC fitness and sensitivity to treatments through a general cellular stress involving endoplasmic reticulum (ER) stress, decreased autophagy, and oxidative stress.[13,24] To determine if such cellular stress occurred in PCs producing LCDD LC, we performed RNA-seq on magnetically

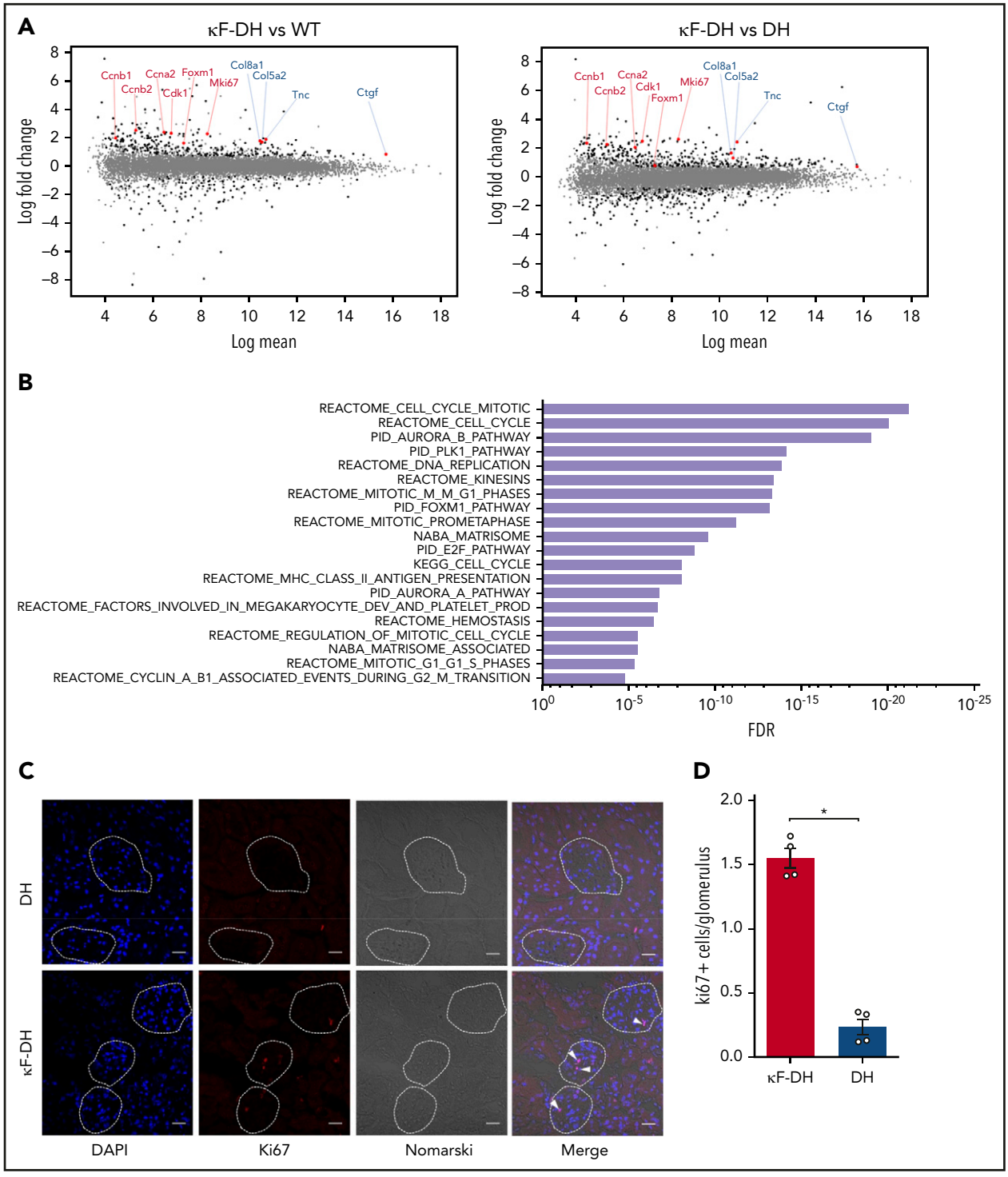

Figure 4. Glomerular transcriptomic analysis of κF-DH. (A) MA plots of normalized transcript values from κF-DH vs WT (left) and κF-DH vs DH (right) glomeruli (n = 4 DH and κF-DH mice and n = 5 WT mice). Examples of overexpressed genes in the cell-cycle (red) and matrisome (blue) pathways are represented. (B) Top 20 enriched pathways based on the C2 canonical pathways from the Molecular Signatures Database (MSignDB v.6.2). All differentially expressed genes in κF-DH compared with both WT and DH glomeruli (supplemental Figure 5A) are included in the analysis (n = 155 upregulated and n = 37 downregulated genes). FDR *q* values of the overlaps are represented on the bar graphs. (C) Intracellular Ki67 staining on frozen kidney sections of κF-DH compared with DH mice; the analysis was performed in 5-month-old mice. Glomeruli are surrounded, and positive cells appear in red (arrowhead). Scale bars, 30 μm. (D) Mean of Ki67 positive cells in glomeruli of complete kidney section of κF-DH compared with DH mice (n = 4 of each strain). Note the increase of Ki67$^+$ cells in κF-DH glomeruli compared with DH mice. Means ± standard error of the mean, and comparisons between 2 groups were calculated using the nonparametric Mann-Whitney test. *$P < .05$.

sorted spleen PCs (>80%) of κF-DH mice compared with WT mice producing polyclonal complete immunoglobulins and with DH mice producing polyclonal FLC. Our data revealed a total of 1946 and 809 expressed genes deregulated in LCDD LC–producing PCs compared with WT and DH controls, respectively (abs[$\log_2$FC] ≥0.7, FDR ≤0.05); among these deregulated genes, 722 and 376 were upregulated and 1224 and 433 were downregulated, respectively (Figure 5A). Only genes similarly deregulated in both comparisons (κF-DH vs WT and κF-DH vs DH) were considered for further analysis (supplemental Figure 7A). This restricted the analysis to 180 and 213 genes, respectively, upregulated and downregulated in κF-DH vs both controls (supplemental Figure 7A-B). C2 canonical pathway analysis (MSignDB v.6.2) found that among upregulated genes, the only significant pathways were related to UPR (Figure 5B; supplemental Table 4). Genes of the UPR pathway upregulated in κF-DH PCs vs each control (WT and DH) are indicated on the MA plots (Figure 5A), showing that they were not only upregulated but, as expected, also highly expressed in PCs.[25] Activated pathways in each comparison are depicted in supplemental Figure 7C. Gene ontology (GO) biologic process analysis showed that 9 of the 20 most significant overlaps and the 3 most significant pathways were related to topologically incorrect proteins and ER stress, further suggesting that the activation of UPR was likely due to the pathogenic LCDD LC (Figure 5C; supplemental Table 5). Downregulated genes were associated with ECM modification, hematopoietic lineage, and G protein–coupled protein signaling (supplemental Table 6). We performed real-time polymerase chain reaction on selected genes (Herpud1, Hspa5, Ddit3, Xbp1s) and confirmed a similar tendency for upregulation of genes involved in UPR, even if, consistent with RNA-seq analysis, no increase in Xbp1s was observed (Figure 5D). We next verified if such ER stress could sensitize PCs to PI.[13] We treated mice with suboptimal doses of bortezomib for 2 consecutive days to evaluate the level of PC depletion. This protocol led to a partial (approximately twofold) reduction of the absolute number of PCs in WT and DH mice (45.16% and 57.54% of depletion, respectively) as previously demonstrated.[13] In contrast, PC depletion in κF-DH mice was far more efficient than in control mice, with a mean depletion of 84.46%, corresponding to a 6.44-fold reduction in absolute PC number (Figure 5E).

Removal of circulating LC leads to rapid decrease in renal LC deposits and protects mice from kidney failure

The efficient response to PI prompted us to evaluate the effect of LC removal on renal lesions evolution. Weekly injections of bortezomib plus cyclophosphamide were administered to 6-month-old mice over 2 months, which were compared with age-matched untreated mice. All mice were subsequently euthanized at the end of the histologic study treatment. The treatment led to an almost complete (>90% of reduction) and sustained depletion of circulating κLC (Figure 6A). Treatment completely protected mice from kidney dysfunction (Figure 6B) and early death (Figure 6C), and treated mice presented significantly fewer abundant renal LC deposits as compared with nontreated mice (Figure 6D-E). Interestingly, number of kidney lesions after treatment (at 8 months) was also significantly lower as compared with younger mice at 6 months (Figure 6D-E). Periodic acid Schiff staining showed glomeruli of smaller size in treated κF-DH mice as compared with 6-month-old mice, and EM analysis revealed less marked glomerulosclerosis and the absence of thrombotic microangiopathy–like lesions, despite persistence of diffuse thickening of glomerular BMs (Figure 6D). Although serum creatinine was significantly increased in nontreated mice associated with an increase of serum FLC, it was maintained at normal levels in treated mice (Figure 6A-B), which, compared with control 6-month-old mice, showed a slight but nonsignificant increase in albuminuria (Figure 6F) and no rise in serum FLC (Figure 6A).

Discussion

We herein describe the first transgenic mouse model fully reproducing specific renal lesions and kidney dysfunction observed in human LCDD. We previously characterized another model of MIDD using a similar transgenic strategy (ie, targeted insertion of a human truncated γ1 HC obtained from a patient with biopsy-proven HCDD into the mouse κ locus).[13] In this model, the pathogenic immunoglobulin induced kidney lesions closely resembling those observed in human MIDD, except glomerulosclerosis, a hallmark of HCDD,[5] and glomerular dysfunction. We first suspected the role of the genetic background (C57/BL6 and 129SV),[26-28] but we could not exclude the possibility that the low level of circulating HC (~30-40 μg/mL) precluded pathologic progression of the disease. In the present LCDD mouse model, we used a new strategy to obtain high levels of circulating human FLC.[14,29] We inserted the pathogenic V domain of human LC into the κ locus and crossed the mice with DH mice, which display increased PC development in the absence of immunoglobulin HC.[14,16,30] Production of chimeric FLC occurred in virtually all PCs, and κLC serum level reached 1 g/L in κF-DH mice, which is similar to that observed in LCDD patients.[19] Similar productions were obtained in other unpublished models of MGRSs,[14] making this strategy a powerful tool to study the pathogenicity of monoclonal LC in vivo.

Accordingly, κF-DH mice recapitulate progressive glomerular lesions closely resembling those observed in MIDD patients, with linear monoclonal κLC deposits along glomerular and tubular BMs and in the mesangium, with glomerular enlargement and mesangial hypercellularity, resulting in albuminuria. The lesions eventually lead to nodular glomerulosclerosis and end-stage kidney failure within the first year. We first confirmed that the V domain alone bore the pathogenic properties of LCCD LC, similarly to what we showed in a model of LC-induced Fanconi syndrome.[15] This does not mean that the C domain could not play a positive or negative role in the deposition process, and it would have been interesting to compare with full-length human LC. Unfortunately, our attempts to obtain such a model with insertion of the complete cDNA in the κ locus were unfruitful, with very low expression of the transgene (unpublished data). Tumor graft models could be advantageously used to compare full-length with chimeric LC or to test V domain mutations that could be involved in the deposition of the LC.[20,31] If the pathologic lesions slowly progress during the first months, the occurrence of kidney dysfunction with increased serum creatinine seems to be more sudden and unpredictable, requiring careful follow-up of mice after month 6. All these features make the κF-DH mice an accurate model to study the pathophysiology of MIDD, as well as other kidney diseases featuring nodular glomerulosclerosis, particularly DN. Indeed, κF-DH mice recapitulate all the criteria used to validate the glomerular lesions

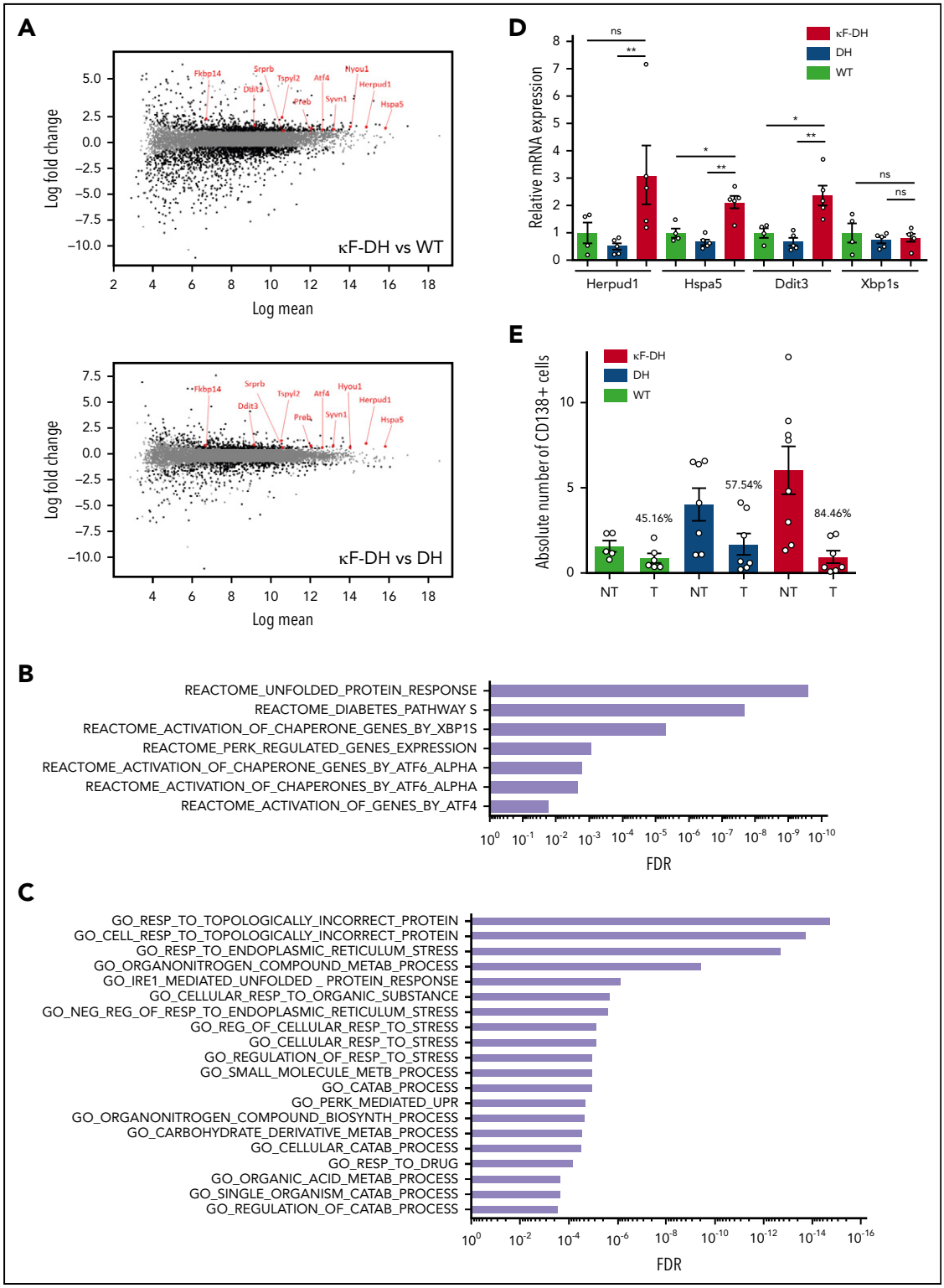

Figure 5. ER stress and sensitivity to PI of κF-DH PCs. (A) MA plots of normalized transcript values from κF-DH vs WT (top) and κF-DH vs DH (bottom) PCs (n = 3 mice of each strain). Overexpressed genes, common in both comparisons, from the REACTOME unfolded protein response (UPR) pathway are represented. (B) Significantly enriched pathways based on the C2 canonical pathways from the Molecular Signature Database (MSignDB v.6.2). Analysis was performed in the 180 upregulated genes in κF-DH vs both controls (WT and DH PCs). FDR *q* values of the overlaps are represented on the bar graphs. (C) GO biological process enrichment analysis. Enrichment was performed in the 180 upregulated genes in κF-DH vs both controls (WT and DH PCs). FDR *q* values of the overlaps are represented on the bar graphs. (D) Quantitative transcriptional analysis of ER stress markers Herpud1, Hspa5, Ddit3, and Xbp1s in sorted CD138$^+$ PCs of κF-DH, DH, and WT mice. Increase of Herpud1, Hspa5, and Ddit3 but not Xbp1s in κF-DH transcripts corroborates the transcriptomic analysis (n = 4 mice of each group). (E) Comparison of the absolute number of splenic CD138$^+$ PCs between PI-treated (T) mice and nontreated (NT) mice. Percentage of depletion for each group is indicated over the bars (n = 5-8 mice of each group in 3 independent experiments). Means ± standard error of the mean, and comparisons between 2 groups were calculated using the nonparametric Mann-Whitney test. *$P < .05$, **$P < .01$. mRNA, messenger RNA; ns, nonsignificant.

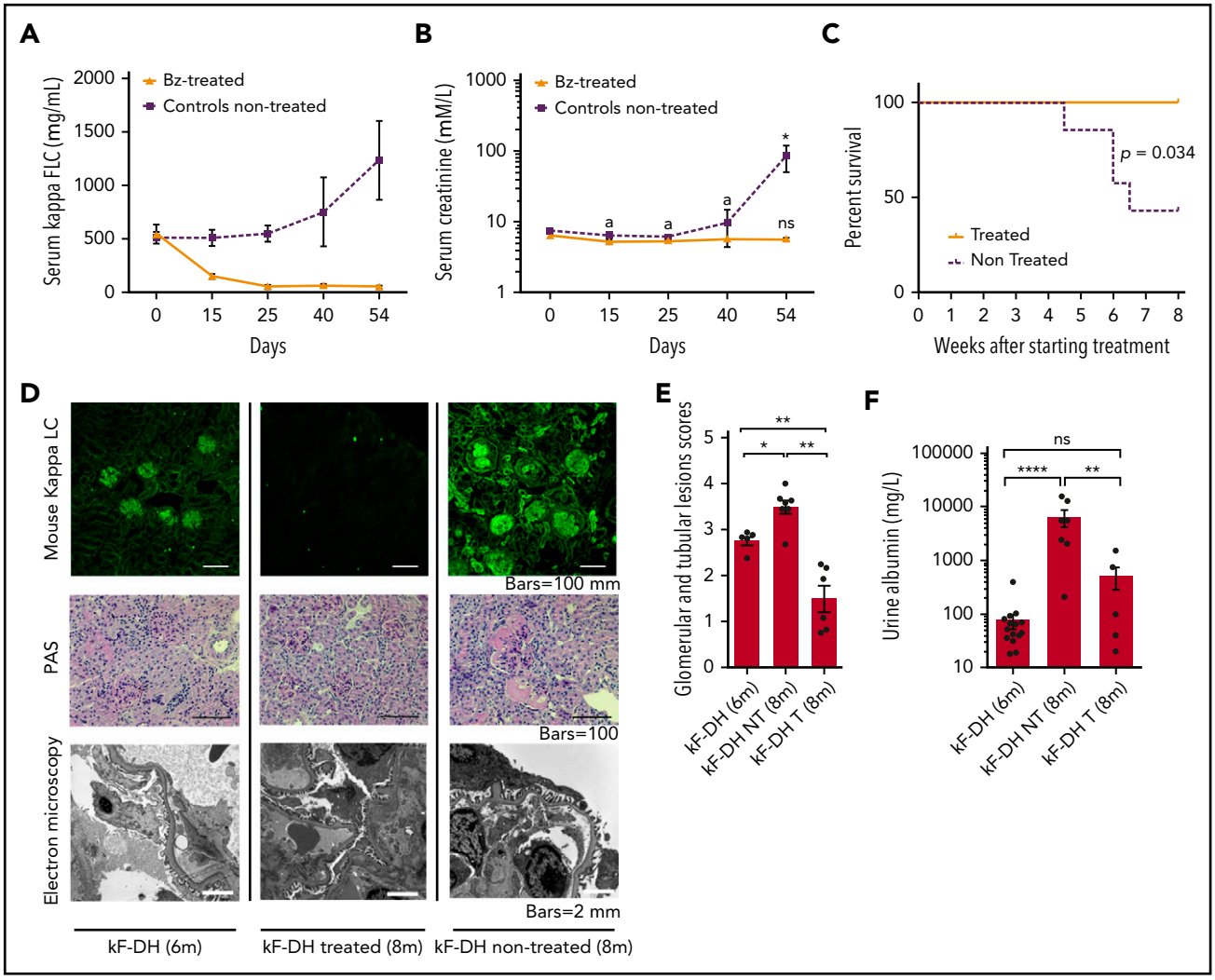

Figure 6. Effect of bortezomib (Bz)/cyclophosphamide–based therapy on survival, renal lesions, and function of kF-DH mice. Serum LC levels (μg/mL) (A) and serum creatinine levels (B) in treated (n = 6) and nontreated (n = 7) κF-DH mice during 8 weeks of treatment. Note the absence of kidney dysfunction in treated mice. Statistics at day 54 compared end of treatment or euthanization with day 0. (C) Kaplan-Meier overall survival analysis of nontreated vs treated kF-DH mice during 8 weeks of treatment (from age 6-8 months). Note that none of the treated mice died during the course of treatment, whereas half of the nontreated control mice died. Results are from 2 independent experiments. (D) Lesion analysis of kidney sections by immunofluorescence microscopy (top), light microscopy (middle), and electron microscopy (bottom) between κF-DH mice at the beginning of treatment and mice treated/nontreated at the end of treatment. Note that deposits revealed by immunofluorescence in nontreated mice or mice at the beginning of treatment totally disappeared in treated mice. LCDD-suggestive lesions are also absent in treated mice (no glomerulosclerosis or thrombotic microangiopathy–like lesions). Original magnification ×200. (E) Comparison of κ LC deposits in kidneys of κF-DH mice at the age at beginning of treatment (6-month-old kF-DH mice, n = 5) and the kidneys of treated and nontreated mice at the end of treatment. Evaluation of total deposits, glomerular and tubular, were performed with anti-mouse κ LC staining by 4 different experimenters (n = 2 blinded experiments). (F) Urine albumin levels in treated (κF-DH T) and nontreated (κF-DH NT) mice at the end of treatment compared with 6-month-old mice (κF-DH). Survival data were analyzed using log-rank (Mantel-Cox) test, and comparisons between 2 groups were calculated using the nonparametric Mann-Whitney test. Means ± standard error of the mean, and only significant *P* values are indicated. All statistics at 8 months corresponded to end of treatment or euthanization at humane end point. **P* < .05, ***P* < .01, *****P* < .0001; n = 3 mice.

of DN as established by the Diabetic Complications Consortium[32] and could be advantageously used to decipher common pathways involved in mesangial cell proliferation and ECM expansion leading to glomerulosclerosis. Nodular glomerulosclerosis has been widely studied, especially in the context of DN[32-34] and LCDD,[8,11,35] highlighting a role for TGFβ signaling and PDGF. However, because of the lack of relevant animal models reproducing the chronic progression of kidney lesions, it is still unclear whether TGFβ and PDGF are early mediators of glomerulosclerosis or if they are involved later, enhancing and accelerating terminal fibrosis of the glomeruli. When we performed RNA-seq on glomeruli from 6-month-old LCDD mice, which display abundant LC deposits but no glomerulosclerosis, we did not find any activation of the TGFβ or PDGF pathway despite already-present ECM deregulation, as indicated by the overexpression of Tnc.[10,12,36] Tnc is a ubiquitous component of the expanded glomerular ECM in pathologic conditions, including DN.[37] More specifically, it has been characterized as a main component of abnormal ECM produced by mesangial cells after LCDD LC but not AL LC exposure, likely because of the concomitant overexpression of matrix metalloproteinases, which degrade ECM components in the latter case.[9,10] We observed a slight but significant increase of CTGF, known for its profibrotic properties in damaged tissues, including the kidney.[23,38] The most prominent early effect of LC deposition in our model was the induction of proliferation, as observed by RNA-seq and Ki67

staining. This result is consistent with the presence of hypercellularity and the enlargement of glomeruli that precede glomerulosclerosis and kidney dysfunction. Similar studies in mice with more advanced disease stages or in treated vs nontreated mice should be carried out to decipher the sequential molecular events leading to glomerulosclerosis, but our results suggest that TGFβ overproduction and its consequences are secondary events after LC-induced proliferation of mesangial cells and production of abnormal ECM. Understanding the pathways linking LC deposition and cellular proliferation should likely provide new insights into the pathophysiology of the disease.

Recent studies have highlighted the efficiency of PI-based treatment in patients with MIDD, as already demonstrated in AL amyloidosis.[5,19,39-42] We confirmed this observation in our mouse model. This regimen led to a rapid hematologic response with almost complete and sustained depletion of circulating FLC, leading to a significant improvement in kidney lesions. Interestingly, kidney lesions were significantly decreased compared with those observed in animals at ages corresponding to the beginning of treatment, highlighting a possible cleaning mechanism leading to the elimination of LC deposits. This improvement in kidney lesions was also characterized by normalization of glomerular size and absence of thrombotic microangiopathy–like lesions occasionally observed in 6-month-old mice. Although complete recovery was not achieved after 2 months as observed by electron microscopy, the treatment was sufficient to maintain normal serum creatinine levels. This result is in accordance with studies of human diseases, including DN,[43,44] showing that glomerulosclerosis at early stages can be reversed with efficient treatment, although this process in humans can take several years. In mouse models, however, the reversibility was demonstrated after short-term treatment in DN[45,46] or hypertension-related glomerulosclerosis.[47] Accordingly, we demonstrated the almost complete reversibility of kidney lesions in LCDD-induced glomerulosclerosis after LC depletion. Additional studies are needed to confirm if long-term LC removal could lead to complete renal recovery to decipher the involved mechanisms and test therapeutic strategies that could accelerate this process. In this latter view, it seems that therapy based on mesenchymal stem cells could be a valuable approach, as demonstrated in rodent models of glomerulopathies[48,49] or more recently in ex vivo models of monoclonal LC-induced glomerular damage.[50] Our model also enabled us to analyze the intrinsic toxicity of pathogenic monoclonal LC for PCs. Similarly to what was shown in patients with MIDD[5,7,19,51] and in the HCDD model,[13] PCs producing LCDD LC are highly sensitive to PI. We assume that mouse PCs are quite different from dysplastic human PCs, in that genomic alterations other than sole LC production could explain such sensitivity. However, in contrast, differences in PI sensitivity in our model uniquely depended on the presence of human LC, because PCs were otherwise strictly identical. We showed that these PCs display a high ER stress and, more generally, an overexpression of genes involved in the response to misfolded or unfolded proteins. Similar results have been obtained with PCs forced to express HC only,[52] truncated HC,[13] or truncated LC.[53] Collectively, we hypothesize that the high sensitivity to PI is likely related to the impaired capacity of PCs to cope with the production of an abnormal, aggregation-prone, monoclonal LC, as observed in AL amyloidosis.[24] Using our transgenic strategy, we now have developed several mouse models expressing human LC from other MGRSs, including AL amyloidosis and Fanconi syndrome,[14] which will serve to determine whether all pathogenic LCs are toxic for PCs and decipher the common pathways leading to ER stress and PI sensitivity.

We describe here the first mouse model fully recapitulating the features of MIDD, including glomeruloslerosis and end-stage kidney disease. Compared with other models of chronic kidney diseases, the development of kidney dysfunction relies on the natural causing factor (ie, monoclonal LC), without any chemical or physical induction or genetic mutations artificially triggering the disease.[54] Consequently, such a model will likely be useful to understand the molecular mechanisms leading to glomerulosclerosis in MIDD, as well as other chronic kidney diseases, such as DN. It also confirms the toxicity of abnormal LC for PCs and will likely serve to design and test new therapeutic strategies for MIDD and other related diseases.

Acknowledgments

The authors thank the staff of the Biologie Intégrative Santé Chimie Environnement (BISCEm) technical platforms at the University of Limoges (animal, cell cytometry, microscopy, transgenesis, and bioinformatics facilities), the Department of Pathology of Poitiers, L. Magnol and K. Vuillier for access to the Konelab 30 analyzer, and A. Garot for helpful discussions.

This work was supported by grants from Fondation Française pour la Recherche contre le Myélome et les Gammapathies Monoclonales, Limousin Committees of Ligue Nationale contre le Cancer, Fondation pour la Recherche Médicale, Agence Régionale de la Santé, and Institut Universitaire de France. S.B. is supported by Centre Hospitalier Universitaire Dupuytren Limoges and Plan National Maladies Rares. M.V.A., A.B., and M.O.A. were funded by fellowships from Région Limousin (now Région Nouvelle Aquitaine), the French Ministry of Research, and Agence de Valorisation de la Recherche de l'Université de Limoges. M.V.A is funded by a fellowship from Fondation ARC pour la Recherche sur le Cancer.

Authorship

Contribution: S.B. designed, performed, and analyzed experiments and drafted the manuscript; M.V.A. performed and analyzed experiments and drafted the manuscript; A.B. designed, performed, and analyzed some experiments; V.J. drafted parts of the manuscript and provided general advice; A.R., S.K., C.C., C.O., Z.O., and M.O.A. performed and analyzed some experiments; F.B., B.H., A.P., and N.P. performed the biostatistics and bioinformatics on RNA-seq data; G.T. analyzed and provided advice on kidney pathology; A.J., L.D., and M.C. provided general advice and reviewed the manuscript; F.B. analyzed data and critically reviewed the manuscript; and C.S. designed and analyzed experiments, supervised research, and wrote the manuscript.

Conflict-of-interest disclosure: The authors declare no competing financial interests.

ORCID profiles: S.B., 0000-0002-8830-955X; A.B., 0000-0002-4153-9171; C.C., 0000-0003-3221-6319; Z.O., 0000-0003-1314-6757; B.H., 0000-0002-2610-8365; M.O.A., 0000-0002-3749-2198; A.J., 0000-0001-7091-8253; L.D., 0000-0002-9480-8515; M.C., 0000-0002-8519-4427; F. Bridoux, 0000-0002-2005-8424; C.S., 0000-0002-1183-4989.

Correspondence: Christophe Sirac, CRIBL Laboratory, UMR CNRS 7276 INSERM 1262, CBRS Room 110, 2 Rue du Dr Marcland, 87000 Limoges, France; e-mail: christophe.sirac@unilim.fr.

Footnotes

Submitted 24 March 2020; accepted 12 May 2020; prepublished online on *Blood* First Edition 19 June 2020. DOI 10.1182/blood.2020005980.

*M.V.A. and A.B. contributed equally to this work.

The online version of this article contains a data supplement.

There is a *Blood* Commentary on this article in this issue.

RNAseq data sets are available at the Gene Expression Omnibus database (accession numbers GSE119049 for glomeruli and GSE119048 for PCs). All data sets can be found in the GEO superseries: GSE119050. The token for full access to GEO data sets is: etopeeysfxsflkl.

The publication costs of this article were defrayed in part by page charge payment. Therefore, and solely to indicate this fact, this article is hereby marked "advertisement" in accordance with 18 USC section 1734.

REFERENCES

1. Leung N, Bridoux F, Hutchison CA, et al; International Kidney and Monoclonal Gammopathy Research Group. Monoclonal gammopathy of renal significance: when MGUS is no longer undetermined or insignificant. *Blood*. 2012;120(22):4292-4295.
2. Bridoux F, Leung N, Hutchison CA, et al; International Kidney and Monoclonal Gammopathy Research Group. Diagnosis of monoclonal gammopathy of renal significance. *Kidney Int*. 2015;87(4):698-711.
3. Preud'homme JL, Aucouturier P, Touchard G, et al. Monoclonal immunoglobulin deposition disease (Randall type). Relationship with structural abnormalities of immunoglobulin chains. *Kidney Int*. 1994;46(4):965-972.
4. Preud'homme JL, Aucouturier P, Touchard G, et al. Monoclonal immunoglobulin deposition disease: a review of immunoglobulin chain alterations. *Int J Immunopharmacol*. 1994; 16(5-6):425-431.
5. Bridoux F, Javaugue V, Bender S, et al. Unravelling the immunopathological mechanisms of heavy chain deposition disease with implications for clinical management. *Kidney Int*. 2017;91(2):423-434.
6. Kaplan B, Livneh A, Gallo G. Charge differences between in vivo deposits in immunoglobulin light chain amyloidosis and non-amyloid light chain deposition disease. *Br J Haematol*. 2007;136(5):723-728.
7. Joly F, Cohen C, Javaugue V, et al. Randall-type monoclonal immunoglobulin deposition disease: novel insights from a nationwide cohort study. *Blood*. 2019;133(6):576-587.
8. Russell WJ, Cardelli J, Harris E, Baier RJ, Herrera GA. Monoclonal light chain–mesangial cell interactions: early signaling events and subsequent pathologic effects. *Lab Invest*. 2001;81(5):689-703.
9. Keeling J, Herrera GA. Matrix metalloproteinases and mesangial remodeling in light chain-related glomerular damage. *Kidney Int*. 2005;68(4):1590-1603.
10. Keeling J, Herrera GA. An in vitro model of light chain deposition disease. *Kidney Int*. 2009;75(6):634-645.
11. Herrera GA, Turbat-Herrera EA, Teng J. Animal models of light chain deposition disease provide a better understanding of nodular glomerulosclerosis. *Nephron*. 2016; 132(2):119-136.
12. Yang CW, Hattori M, Vlassara H, et al. Overexpression of transforming growth factor-beta 1 mRNA is associated with up-regulation of glomerular tenascin and laminin gene expression in nonobese diabetic mice. *J Am Soc Nephrol*. 1995;5(8):1610-1617.
13. Bonaud A, Bender S, Touchard G, et al. A mouse model recapitulating human monoclonal heavy chain deposition disease evidences the relevance of proteasome inhibitor therapy. *Blood*. 2015;126(6):757-765.
14. Sirac C, Herrera GA, Sanders PW, et al. Animal models of monoclonal immunoglobulin-related renal diseases. *Nat Rev Nephrol*. 2018; 14(4):246-264.
15. Sirac C, Bridoux F, Carrion C, et al. Role of the monoclonal kappa chain V domain and reversibility of renal damage in a transgenic model of acquired Fanconi syndrome. *Blood*. 2006;108(2):536-543.
16. Casola S, Otipoby KL, Alimzhanov M, et al. B cell receptor signal strength determines B cell fate. *Nat Immunol*. 2004;5(3):317-327.
17. Neubert K, Meister S, Moser K, et al. The proteasome inhibitor bortezomib depletes plasma cells and protects mice with lupus-like disease from nephritis. *Nat Med*. 2008;14(7): 748-755.
18. Takemoto M, Asker N, Gerhardt H, et al. A new method for large scale isolation of kidney glomeruli from mice. *Am J Pathol*. 2002; 161(3):799-805.
19. Cohen C, Royer B, Javaugue V, et al. Bortezomib produces high hematological response rates with prolonged renal survival in monoclonal immunoglobulin deposition disease. *Kidney Int*. 2015;88(5):1135-1143.
20. Khamlichi AA, Rocca A, Touchard G, Aucouturier P, Preud'homme JL, Cogné M. Role of light chain variable region in myeloma with light chain deposition disease: evidence from an experimental model. *Blood*. 1995; 86(10):3655-3659.
21. Subramanian A, Tamayo P, Mootha VK, et al. Gene set enrichment analysis: a knowledge-based approach for interpreting genome-wide expression profiles. *Proc Natl Acad Sci USA*. 2005;102(43):15545-15550.
22. Liberzon A, Birger C, Thorvaldsdóttir H, Ghandi M, Mesirov JP, Tamayo P. The Molecular Signatures Database (MSigDB) hallmark gene set collection. *Cell Syst*. 2015;1(6): 417-425.
23. Gupta S, Clarkson MR, Duggan J, Brady HR. Connective tissue growth factor: potential role in glomerulosclerosis and tubulointerstitial fibrosis. *Kidney Int*. 2000;58(4):1389-1399.
24. Oliva L, Orfanelli U, Resnati M, et al. The amyloidogenic light chain is a stressor that sensitizes plasma cells to proteasome inhibitor toxicity. *Blood*. 2017;129(15):2132-2142.
25. Tellier J, Shi W, Minnich M, et al. Blimp-1 controls plasma cell function through the regulation of immunoglobulin secretion and the unfolded protein response. *Nat Immunol*. 2016;17(3):323-330.
26. Zheng F, Striker GE, Esposito C, Lupia E, Striker LJ. Strain differences rather than hyperglycemia determine the severity of glomerulosclerosis in mice. *Kidney Int*. 1998; 54(6):1999-2007.
27. Ma L-J, Fogo AB. Model of robust induction of glomerulosclerosis in mice: importance of genetic background. *Kidney Int*. 2003;64(1): 350-355.
28. Qi Z, Fujita H, Jin J, et al. Characterization of susceptibility of inbred mouse strains to diabetic nephropathy. *Diabetes*. 2005;54(9): 2628-2637.
29. Sirac C, Bender S, Jaccard A, et al. Strategies to model AL amyloidosis in mice [published correction appears in *Amyloid*. 2011;18(suppl 1):47]. *Amyloid*. 2011;18(suppl 1):45-47.
30. Lechouane F, Bonaud A, Delpy L, et al. B-cell receptor signal strength influences terminal differentiation. *Eur J Immunol*. 2013;43(3): 619-628.
31. Decourt C, Rocca A, Bridoux F, et al. Mutational analysis in murine models for myeloma-associated Fanconi's syndrome or cast myeloma nephropathy. *Blood*. 1999; 94(10):3559-3566.
32. Brosius FC III, Alpers CE, Bottinger EP, et al; Animal Models of Diabetic Complications Consortium. Mouse models of diabetic nephropathy. *J Am Soc Nephrol*. 2009;20(12): 2503-2512.
33. Chen S, Jim B, Ziyadeh FN. Diabetic nephropathy and transforming growth factor-beta: transforming our view of glomerulosclerosis and fibrosis build-up. *Semin Nephrol*. 2003;23(6):532-543.
34. Hu C, Sun L, Xiao L, et al. Insights into the mechanisms involved in the expression and regulation of extracellular matrix proteins in diabetic nephropathy. *Curr Med Chem*. 2015; 22(24):2858-2870.
35. Zhu L, Herrera GA, Murphy-Ullrich JE, Huang ZQ, Sanders PW. Pathogenesis of glomerulosclerosis in light chain deposition disease. Role for transforming growth factor-beta. *Am J Pathol*. 1995;147(2):375-385.
36. Fu H, Tian Y, Zhou L, et al. Tenascin-C is a major component of the fibrogenic niche in kidney fibrosis. *J Am Soc Nephrol*. 2017;28(3): 785-801.
37. Truong LD, Pindur J, Barrios R, et al. Tenascin is an important component of the glomerular extracellular matrix in normal and pathologic conditions. *Kidney Int*. 1994;45(1):201-210.
38. Sonnylal S, Shi-Wen X, Leoni P, et al. Selective expression of connective tissue growth factor in fibroblasts in vivo promotes systemic tissue fibrosis. *Arthritis Rheum*. 2010;62(5): 1523-1532.
39. Kastritis E, Wechalekar AD, Dimopoulos MA, et al. Bortezomib with or without dexamethasone in primary systemic (light chain) amyloidosis. *J Clin Oncol*. 2010;28(6):1031-1037.

40. Jaccard A, Comenzo RL, Hari P, et al. Efficacy of bortezomib, cyclophosphamide and dexamethasone in treatment-naïve patients with high-risk cardiac AL amyloidosis (Mayo Clinic stage III). *Haematologica*. 2014;99(9):1479-1485.

41. Reece DE, Hegenbart U, Sanchorawala V, et al. Long-term follow-up from a phase 1/2 study of single-agent bortezomib in relapsed systemic AL amyloidosis. *Blood*. 2014;124(16):2498-2506.

42. Patel K, Dillon JJ, Leung N, et al. Use of bortezomib in heavy-chain deposition disease: a report of 3 cases. *Am J Kidney Dis*. 2014;64(1):123-127.

43. Fioretto P, Steffes MW, Sutherland DE, Goetz FC, Mauer M. Reversal of lesions of diabetic nephropathy after pancreas transplantation. *N Engl J Med*. 1998;339(2):69-75.

44. Yang H-C, Fogo AB. Mechanisms of disease reversal in focal and segmental glomerulosclerosis. *Adv Chronic Kidney Dis*. 2014;21(5):442-447.

45. Pichaiwong W, Hudkins KL, Wietecha T, et al. Reversibility of structural and functional damage in a model of advanced diabetic nephropathy. *J Am Soc Nephrol*. 2013;24(7):1088-1102.

46. Conway BR, Betz B, Sheldrake TA, et al. Tight blood glycaemic and blood pressure control in experimental diabetic nephropathy reduces extracellular matrix production without regression of fibrosis. *Nephrology (Carlton)*. 2014;19(12):802-813.

47. Aldigier JC, Kanjanbuch T, Ma L-J, Brown NJ, Fogo AB. Regression of existing glomerulosclerosis by inhibition of aldosterone. *J Am Soc Nephrol*. 2005;16(11):3306-3314.

48. Kunter U, Rong S, Djuric Z, et al. Transplanted mesenchymal stem cells accelerate glomerular healing in experimental glomerulonephritis. *J Am Soc Nephrol*. 2006;17(8):2202-2212.

49. Lv S, Liu G, Sun A, et al. Mesenchymal stem cells ameliorate diabetic glomerular fibrosis in vivo and in vitro by inhibiting TGF-β signalling via secretion of bone morphogenetic protein 7. *Diab Vasc Dis Res*. 2014;11(4):251-261.

50. Herrera GA, Teng J, Zeng C, et al. Phenotypic plasticity of mesenchymal stem cells is crucial for mesangial repair in a model of immunoglobulin light chain-associated mesangial damage. *Ultrastruct Pathol*. 2018;42(3):262-288.

51. Kastritis E, Migkou M, Gavriatopoulou M, Zirogiannis P, Hadjikonstantinou V, Dimopoulos MA. Treatment of light chain deposition disease with bortezomib and dexamethasone. *Haematologica*. 2009;94(2):300-302.

52. Zhou P, Ma X, Iyer L, Chaulagain C, Comenzo RL. One siRNA pool targeting the λ constant region stops λ light-chain production and causes terminal endoplasmic reticulum stress. *Blood*. 2014;123(22):3440-3451.

53. Srour N, Chemin G, Tinguely A, et al. A plasma cell differentiation quality control ablates B cell clones with biallelic Ig rearrangements and truncated Ig production. *J Exp Med*. 2016;213(1):109-122.

54. Betz B, Conway BR. An update on the use of animal models in diabetic nephropathy research. *Curr Diab Rep*. 2016;16(2):18.